Propagation of radially polarized Hermite non-uniformly correlated beams in a turbulent atmosphere

SHUQIN LIN,[1] CONG WANG,[1] XINLEI ZHU,[2] RONG LIN,[1,3] FEI WANG,[2] GREG GBUR,[4,5] YANGJIAN CAI,[1,2,6] AND JIAYI YU[1,7]

[1] *Shandong Provincial Engineering and Technical Center of Light Manipulations & Shandong Provincial Key Laboratory of Optics and Photonic Device, School of Physics and Electronics, Shandong Normal University, Jinan 250014, China*
[2] *School of Physical Science and Technology, Soochow University, Suzhou 215006, China*
[3] *College of Physics and Electronic Engineering, Heze University, Heze 274015, China*
[4] *Department of Physics and Optical Science, University of North Carolina at Charlotte, Charlotte, North Carolina 28223, USA*
[5] *gjgbur@uncc.edu*
[6] *yangjiancai@suda.edu.cn*
[7] *jiayiyu0528@sdnu.edu.cn*

Abstract: We study the propagation properties of a recently introduced class of structured beams, radially polarized Hermite non-uniformly correlated (RPHNUC) beams, in a turbulent atmosphere using the extended Huygens-Fresnel integral and investigate how the mode order and coherence width play a role in resisting the degradation and depolarization effects of the turbulence. In contrast with conventional vector partially coherent beams (PCBs) with uniform (Schell-model) correlation structure, the interaction of the non-uniform correlation structure and non-uniform polarization gives these beams the ability to self-heal their intensity distribution and polarization over certain propagation ranges in turbulence. These properties suggest that RPHNUC beams may be useful in a number of applications, in particular optical trapping and free-space optical communications.

1. Introduction

Due to its brightness, directionality, and monochromaticity, coherent laser light has been widely used in military defense, medicine, industrial processing, optical communication systems and other fields, playing a vital role in human social progress and economic development [1–5]. Free space optical (FSO) communications is one of the leading laser applications, and compared with traditional radio communications technology, it has many advantages. However, over significant propagation distances, the laser beam will experience random wavefront fluctuations due to atmospheric turbulence, leading to beam wander and intensity scintillation. This increases the signal data error rate at the receiving end, limiting the performance of the communication systems [6]. Therefore, it is of great scientific and practical importance to study how to reduce the negative effects of atmospheric turbulence on laser beams.

It is now well-known that adjusting the coherence of structured beams is an important strategy to improve the performance of laser beams in turbulence [7,8] and it is also a strategy to encode information into the degrees of coherence for transmission [9]. In particular, laser beams with low spatial coherence, labeled partially coherent beams (PCBs) [8], have lower turbulence-induced negative effects than their fully coherent counterparts [6,10–13]. This resistance has been physically explained from the perspective of the coherent mode representation [14,15], which indicates that light is sent simultaneously through distinct non-interfering channels. Laser beams with a Gaussian Schell-model degree of coherence, with a homogeneous (uniform) correlation

structure, are the most familiar kind of PCBs and their propagation properties in free space and turbulence have been studied extensively. However, since Gori *et al.* introduced a new method for designing PCBs with novel correlation structures [16,17], lots of effort has been focused on investigating the extraordinary propagation properties and increased resistance to turbulent atmosphere of beams with these new correlations. Among the papers that have been published since then include works on Laguerre-Gaussian correlated Schell-model beams, optical coherence lattices, and Hermite-Gaussian correlated Schell-model beams. Such beams exhibit many extraordinary, potentially beneficial properties and excellent resistance to turbulence on propagation [18–22].

The aforementioned works focus on Schell-model sources, leaving many possible states of spatial coherence unexplored. Another broad and extremely important class derived from the formalism by Gori *et al.* is a spatially variant correlation function, i.e., non-uniformly correlated (NUC) beams [23–28]. PCBs with non-uniform correlation structure display self-focusing and self-shifting properties and it was shown that such beams can have, under certain circumstances, not only lower scintillation but higher intensity than Gaussian Schell-model beams in turbulence. Thus, NUC beams achieve both high intensity and low scintillation, especially desirable when laser beams are used in FSO communications.

Polarization is also an important property of laser beams and manipulating polarization is also an effective strategy to improve turbulence resistance of beams [29–31]. The effects of polarization on the statistical properties of beams on propagation in turbulence, especially those with non-uniform polarization (known as vector beams), have been studied extensively. In particular, Gu *et al.* theoretically studied the scintillation of spatially coherent non-uniformly polarized beams in turbulence, and found that such beams can reduce the scintillation through polarization effects alone [29]; these results were confirmed by experiment [31].

The combination of polarization and coherence leads beams to have even better resistance to turbulence. In particular, Wang *et al.* reported the scintillation of radially polarized PCBs in turbulence [32]. Such beams have advantage for reducing turbulence-induced scintillation than PCBs with uniform polarization. Additional studies have reported that the combination of polarization and coherence can further reduce the negative effects induced by atmospheric turbulence [33–36]. However, the aforementioned research focuses on the atmospheric propagation properties of laser beams with polarization and uniform (Schell-model) correlation structure. Little is known about the study of the propagation characteristics of beams with a combination of polarization and non-uniform correlation structure. Thus, in this paper, our aim is to explore the unusual propagation properties and resistance to turbulence of such beams, focusing on the specific example of radially polarized Hermite non-uniformly correlated (RPHNUC) sources, which were recently introduced [28].

2. Beam model and the formulas of RPHNUC beams propagation in turbulence

We do our study using coherence theory in the space-frequency domain, using the cross-spectral density (CSD) matrix as the fundamental quantity characterizing the coherence and polarization of the field. Using a Cartesian coordinate system, the CSD matrix of RPHNUC beams in the source plane is expressed as,

$$\overleftrightarrow{\mathbf{W}}(\mathbf{r}_1, \mathbf{r}_2) = \begin{bmatrix} W_{xx}(\mathbf{r}_1, \mathbf{r}_2) & W_{xy}(\mathbf{r}_1, \mathbf{r}_2) \\ W_{yx}(\mathbf{r}_1, \mathbf{r}_2) & W_{yy}(\mathbf{r}_1, \mathbf{r}_2) \end{bmatrix}, \tag{1}$$

where $W_{\alpha\beta}(\mathbf{r}_1, \mathbf{r}_2) (\alpha, \beta = x, y)$ are the elements of the CSD matrix of RPHNUC beams in the source plane,

$$W_{\alpha\beta}(\mathbf{r}_1, \mathbf{r}_2) = \frac{\alpha_1 \beta_2}{4\omega_0^2} \exp\left(-\frac{\mathbf{r}_1^2 + \mathbf{r}_2^2}{4\omega_0^2}\right) \mu_{\alpha\beta}(\mathbf{r}_1, \mathbf{r}_2), \tag{2}$$

and $\mu_{\alpha\beta}(\mathbf{r}_1, \mathbf{r}_2)$ represents the degree of coherence of RPHNUC beams [28],

$$\mu_{\alpha\beta}(\mathbf{r}_1, \mathbf{r}_2) = G_0 \exp\left[-\frac{(\mathbf{r}_1^2 - \mathbf{r}_2^2)^2}{r_c^4}\right] H_{2m}\left(\frac{\mathbf{r}_1^2 - \mathbf{r}_2^2}{r_c^2}\right), \tag{3}$$

with r_c the coherence width, $G_0 = 1/H_{2m}(0)$ a normalizing constant and $H_{2m}(x)$ denotes the Hermite polynomial of order $2m$.

The propagation of PCBs from the source plane $z = 0$ into an arbitrary plane $z > 0$ in a turbulent medium, under the paraxial approximation, can be described by the extended Huygens-Fresnel principle [5],

$$W_{\alpha\beta}(\boldsymbol{\rho}_1, \boldsymbol{\rho}_2, z) = \left(\frac{k}{2\pi z}\right)^2 \iint_{-\infty}^{\infty} W_{\alpha\beta}(\mathbf{r}_1, \mathbf{r}_2) \exp\left[-\frac{ik}{2z}(\mathbf{r}_1 - \boldsymbol{\rho}_1)^2 + \frac{ik}{2z}(\mathbf{r}_2 - \boldsymbol{\rho}_2)^2\right]$$
$$\times \langle \exp\left[\Psi(\mathbf{r}_1, \boldsymbol{\rho}_1) + \Psi^*(\mathbf{r}_2, \boldsymbol{\rho}_2)\right]\rangle d^2\mathbf{r}_1 d^2\mathbf{r}_2, \tag{4}$$

where $W_{\alpha\beta}(\mathbf{r}_1, \mathbf{r}_2)$ and $W_{\alpha\beta}(\boldsymbol{\rho}_1, \boldsymbol{\rho}_2, z)$ denote the elements of the CSD matrix of the beams in the source and target plane, and $\Psi(\mathbf{r}, \boldsymbol{\rho})$ denotes the complex phase perturbation induced by the refractive-index fluctuations of the random medium between $\mathbf{r}$ and $\boldsymbol{\rho}$. The last term in Eq. (4) can be expressed as [5]

$$\langle \exp\left[\Psi(\mathbf{r}_1, \boldsymbol{\rho}_1) + \Psi^*(\mathbf{r}_2, \boldsymbol{\rho}_2)\right]\rangle$$
$$= \exp\left\{-4\pi^2 k^2 z \int_0^1 \int_0^{\infty} \kappa \Phi_n(\kappa) \cdot \{1 - J_0\left[|(1-\xi)\boldsymbol{P} + \xi\boldsymbol{Q}|\kappa\right]\} d^2\kappa d\xi\right\}, \tag{5}$$

where $\boldsymbol{P} = \boldsymbol{\rho}_1 - \boldsymbol{\rho}_2$, $\boldsymbol{Q} = \mathbf{r}_1 - \mathbf{r}_2$, J_0 is the Bessel function of zero order and can be approximated as

$$J_0\left[|(1-\xi)\boldsymbol{P} + \xi\boldsymbol{Q}|\kappa\right] \sim 1 - \frac{1}{4}\left[(1-\xi)\boldsymbol{P} + \xi\boldsymbol{Q}\right]^2 \kappa^2. \tag{6}$$

On substituting from the relation (6) into Eq. (5), we have

$$\langle \exp\left[\Psi(\mathbf{r}_1, \boldsymbol{\rho}_1) + \Psi^*(\mathbf{r}_2, \boldsymbol{\rho}_2)\right]\rangle$$
$$= \exp\left\{-\left(\frac{\pi^2 k^2 z}{3}\right)\left[(\boldsymbol{\rho}_1 - \boldsymbol{\rho}_2)^2 + (\boldsymbol{\rho}_1 - \boldsymbol{\rho}_2) \cdot (\mathbf{r}_1 - \mathbf{r}_2) + (\mathbf{r}_1 - \mathbf{r}_2)^2\right]\int_0^{\infty} \kappa^3 \Phi_n(\kappa) d^2\kappa\right\}, \tag{7}$$

where $\Phi_n(\kappa)$ is the spatial power spectrum of the refractive-index fluctuations of the turbulent atmosphere.

Now, we may calculate the CSD matrix elements of RPHNUC beams in the target plane by inserting from Eqs. (2) and (3) and (7) into Eq. (4), however, there are higher-order terms in the CSD matrix of such beams and it is too difficult to calculate directly by the traditional method of integration of Eq. (4). Expressing the beam model as the non-negtive definite kernel in one-dimensional integral form introduced by Gori *et al* (see Eq. (3) in Ref. [28]) and then interchanging the orders of the integrals, we obtain the formula

$$W_{\alpha\beta}(\boldsymbol{\rho}_1, \boldsymbol{\rho}_2, z) = \int p_{\alpha\beta}(v) P_{\alpha\beta}(\boldsymbol{\rho}_1, \boldsymbol{\rho}_2, v, z) dv, \tag{8}$$

where $P_{\alpha\beta}(\boldsymbol{\rho}_1, \boldsymbol{\rho}_2, v, z)$ is defined as

$$P_{\alpha\beta}(\boldsymbol{\rho}_1, \boldsymbol{\rho}_2, v, z) = \left(\frac{k}{2\pi z}\right)^2 \iint_{-\infty}^{\infty} V_\alpha^*(\mathbf{r}_1, v) V_\beta(\mathbf{r}_2, v) \exp\left\{-\frac{ik}{2z}\left[(\mathbf{r}_1 - \boldsymbol{\rho}_1)^2 - (\mathbf{r}_2 - \boldsymbol{\rho}_2)^2\right]\right\}$$
$$\times \exp\left\{-\frac{\pi^2 k^2 z}{3}\left[(\boldsymbol{\rho}_1 - \boldsymbol{\rho}_2)^2 + (\boldsymbol{\rho}_1 - \boldsymbol{\rho}_2) \cdot (\mathbf{r}_1 - \mathbf{r}_2) + (\mathbf{r}_1 - \mathbf{r}_2)^2\right]\int_0^{\infty} \kappa^3 \Phi_n(\kappa) d^2\kappa\right\} d^2\mathbf{r}_1 d^2\mathbf{r}_2. \tag{9}$$

and $V_{\alpha(\beta)}(\mathbf{r}, v)$ are the arbitrary kernel and $p_{\alpha\beta}(v)$ are the elements of the weighting matrix as shown in Eq. (6) and Eq. (10) in Ref. [28].

After a lengthy integral calculation, one obtains

$$
P_{jj}(\boldsymbol{\rho}, v, z) = \frac{k^2}{16z^2 w_0^2 \left(|\xi|^2 - \zeta^2\right)} \exp\left(-\frac{k^2}{4\xi z^2}\rho^2\right) \exp\left[-\frac{k^2(\zeta-\xi)^2}{4\xi z^2\left(|\xi|^2-\zeta^2\right)}\rho^2\right]
$$

$$
\times \left\{ \frac{\zeta}{2\left(|\xi|^2-\zeta^2\right)} - \frac{k^2(\zeta-\xi)}{4\xi z^2\left(|\xi|^2-\zeta^2\right)} \left[1 + \frac{\left(\zeta^2-\xi\zeta\right)}{\left(|\xi|^2-\zeta^2\right)}\right] \rho_j^2 \right\}, (j=x,y) \tag{10}
$$

$$
P_{xy}(\boldsymbol{\rho}, v, z) = \frac{k^4(\zeta-\xi^*)(\zeta-\xi)\rho_x\rho_y}{64z^4 w_0^2\left(|\xi|^2-\zeta^2\right)^3} \exp\left(-\frac{k^2}{4\xi^* z^2}\rho_x^2 - \frac{k^2}{4\xi z^2}\rho_y^2\right)
$$

$$
\times \exp\left[-\frac{k^2(\zeta-\xi^*)^2}{4\xi^* z^2\left(|\xi|^2-\zeta^2\right)}\rho_x^2 - \frac{k^2(\zeta-\xi)^2}{4\xi z^2\left(|\xi|^2-\zeta^2\right)}\rho_y^2\right], \tag{11}
$$

$$
P_{yx}(\boldsymbol{\rho}, v, z) = P_{xy}^*(\boldsymbol{\rho}, v, z), \tag{12}
$$

where ρ_x and ρ_y denote the coordinate component in the x and y direction, respectively, and

$$
\xi = \frac{1}{4w_0^2} - ik\left(v - \frac{1}{2z}\right) + \zeta; \quad \zeta = \frac{1}{3}\pi^2 k^2 z \int_0^\infty \kappa^3 \Phi_n(\kappa) d^2\kappa. \tag{13}
$$

We obtain the CSD matrix of RPHNUC beams after propagation by evaluating the integral Eq. (8). One obtains the spectral intensity of RPHNUC beams in the output plane from the expression,

$$
S(\boldsymbol{\rho}, z) = W_{xx}(\boldsymbol{\rho}, \boldsymbol{\rho}, z) + W_{yy}(\boldsymbol{\rho}, \boldsymbol{\rho}, z) = S_{xx}(\boldsymbol{\rho}, z) + S_{yy}(\boldsymbol{\rho}, z). \tag{14}
$$

One obtains the degree of polarization (DOP) of RPHNUC beams in the output plane from the expression,

$$
P(\boldsymbol{\rho}, z) = \sqrt{1 - \frac{4\mathrm{Det}\left[\overleftrightarrow{W}(\boldsymbol{\rho}, \boldsymbol{\rho}, z)\right]}{\left\{\mathrm{Tr}\left[\overleftrightarrow{W}(\boldsymbol{\rho}, \boldsymbol{\rho}, z)\right]\right\}^2}}. \tag{15}
$$

The state of polarization (SOP) of vector PCBs can be characterized by the generalized Stokes parameters or the polarization ellipse [37]. For vector PCBs, it is known that its CSD matrix can be locally represented as a sum of a completely unpolarized portion and a completely polarized portion [37,38], i.e.

$$
\overleftrightarrow{W}(\boldsymbol{\rho}, \boldsymbol{\rho}, z) = \overleftrightarrow{W}^{(u)}(\boldsymbol{\rho}, \boldsymbol{\rho}, z) + \overleftrightarrow{W}^{(p)}(\boldsymbol{\rho}, \boldsymbol{\rho}, z), \tag{16}
$$

where

$$
\overleftrightarrow{W}^{(u)}(\boldsymbol{\rho}, \boldsymbol{\rho}, z) = \begin{pmatrix} A(\boldsymbol{\rho}, \boldsymbol{\rho}, z) & 0 \\ 0 & A(\boldsymbol{\rho}, \boldsymbol{\rho}, z) \end{pmatrix}, \tag{17}
$$

$$
\overleftrightarrow{W}^{(p)}(\boldsymbol{\rho}, \boldsymbol{\rho}, z) = \begin{pmatrix} B(\boldsymbol{\rho}, \boldsymbol{\rho}, z) & D(\boldsymbol{\rho}, \boldsymbol{\rho}, z) \\ D^*(\boldsymbol{\rho}, \boldsymbol{\rho}, z) & C(\boldsymbol{\rho}, \boldsymbol{\rho}, z) \end{pmatrix}, \tag{18}
$$

and

$$
A(\boldsymbol{\rho}, \boldsymbol{\rho}, z) = \frac{1}{2}\left[W_{xx}(\boldsymbol{\rho}, \boldsymbol{\rho}, z) + W_{yy}(\boldsymbol{\rho}, \boldsymbol{\rho}, z)\right.
$$

$$
\left. -\sqrt{\left[W_{xx}(\boldsymbol{\rho}, \boldsymbol{\rho}, z) - W_{yy}(\boldsymbol{\rho}, \boldsymbol{\rho}, z)\right]^2 + 4\left|W_{xy}(\boldsymbol{\rho}, \boldsymbol{\rho}, z)\right|^2}\right], \tag{19}
$$

$$B(\boldsymbol{\rho}, \boldsymbol{\rho}, z) = \frac{1}{2} \left[W_{xx}(\boldsymbol{\rho}, \boldsymbol{\rho}, z) - W_{yy}(\boldsymbol{\rho}, \boldsymbol{\rho}, z) \right.$$
$$\left. + \sqrt{\left[W_{xx}(\boldsymbol{\rho}, \boldsymbol{\rho}, z) - W_{yy}(\boldsymbol{\rho}, \boldsymbol{\rho}, z) \right]^2 + 4 \left| W_{xy}(\boldsymbol{\rho}, \boldsymbol{\rho}, z) \right|^2} \right], \tag{20}$$

$$C(\boldsymbol{\rho}, \boldsymbol{\rho}, z) = \frac{1}{2} \left[W_{yy}(\boldsymbol{\rho}, \boldsymbol{\rho}, z) - W_{xx}(\boldsymbol{\rho}, \boldsymbol{\rho}, z) \right.$$
$$\left. + \sqrt{\left[W_{xx}(\boldsymbol{\rho}, \boldsymbol{\rho}, z) - W_{yy}(\boldsymbol{\rho}, \boldsymbol{\rho}, z) \right]^2 + 4 \left| W_{xy}(\boldsymbol{\rho}, \boldsymbol{\rho}, z) \right|^2} \right], \tag{21}$$

$$D(\boldsymbol{\rho}, \boldsymbol{\rho}, z) = W_{xy}(\boldsymbol{\rho}, \boldsymbol{\rho}, z). \tag{22}$$

The spectral intensities of the completely polarized portion and the completely unpolarized portion are given as

$$S^{(p)}(\boldsymbol{\rho}, z) = \mathrm{Tr} \overleftrightarrow{W}^{(p)}(\boldsymbol{\rho}, \boldsymbol{\rho}, z), \quad S^{(u)}(\boldsymbol{\rho}, z) = \mathrm{Tr} \overleftrightarrow{W}^{(u)}(\boldsymbol{\rho}, \boldsymbol{\rho}, z). \tag{23}$$

The SOP of the completely polarized portion can be characterized by the polarization ellipse. The major and minor semi-axes of the ellipse, A_1 and A_2, as well as its degree of ellipticity, ε, and its orientation angle, θ, are related to the elements of the CSD matrix $\overleftrightarrow{W}(\boldsymbol{\rho}, \boldsymbol{\rho})$ by the following relations [38],

$$A_{1,2}(\boldsymbol{\rho}) = \frac{1}{\sqrt{2}} \left[\sqrt{\left(W_{xx}(\boldsymbol{\rho}, \boldsymbol{\rho}) - W_{yy}(\boldsymbol{\rho}, \boldsymbol{\rho}) \right)^2 + 4 \left| W_{xy}(\boldsymbol{\rho}, \boldsymbol{\rho}) \right|^2} \right.$$
$$\left. \pm \sqrt{\left(W_{xx}(\boldsymbol{\rho}, \boldsymbol{\rho}) - W_{yy}(\boldsymbol{\rho}, \boldsymbol{\rho}) \right)^2 + 4 \left[\mathrm{Re} W_{xy}(\boldsymbol{\rho}, \boldsymbol{\rho}) \right]^2} \right]^{1/2}, \tag{24}$$

$$\theta(\boldsymbol{\rho}) = \frac{1}{2} \arctan \left[\frac{2 \mathrm{Re} \left[W_{xy}(\boldsymbol{\rho}, \boldsymbol{\rho}) \right]}{W_{xx}(\boldsymbol{\rho}, \boldsymbol{\rho}) - W_{yy}(\boldsymbol{\rho}, \boldsymbol{\rho})} \right], \tag{25}$$

$$\varepsilon(\boldsymbol{\rho}) = \frac{A_2(\boldsymbol{\rho})}{A_1(\boldsymbol{\rho})}. \tag{26}$$

In Eq. (24), the signs " + " and " − " between the two roots correspond to A_1 and A_2, respectively.

With the above formulas, one can explore the propagation properties of RPHNUC beams in the turbulent atmosphere. Under the condition of $\Phi_n = 0$, our formulas reduce to those of RPHNUC beams in free space, which we have discussed in Ref. [28].

3. Propagation properties of RPHNUC beams in turbulence

Using the expressions we derived above, we next study the propagation properties of RPHNUC beams in turbulence. In the following numerical examples, we assume that the turbulence obeys Kolmogorov statistics and we adopt the von Karman spectrum for the power spectrum of the index-of-refraction fluctuations of the atmospheric turbulence, which is expressed as [39]

$$\Phi_n(\boldsymbol{\kappa}) = 0.033 C_n^2 \left(\kappa^2 + \kappa_0^2 \right)^{-11/6} \exp \left(-\kappa^2 / \kappa_m^2 \right), \tag{27}$$

where C_n^2 is a generalized refractive-index structure parameter, $\kappa_0 = 2\pi/L_0$ and $\kappa_m = 5.92/l_0$ with L_0 and l_0 being the outer and inner scale of turbulence. The parameters of the beams and the turbulence are set as $w_0 = 1\mathrm{cm}$, $\lambda = 632.8\mathrm{nm}$, $C_n^2 = 5 \times 10^{-15}\mathrm{m}^{-2/3}$, $L_0 = 1\mathrm{m}$ and $l_0 = 1\mathrm{mm}$. For these parameters, the Rytov variance at d km satisfies the expession $\sigma^2 = 0.283 d^{11/6}$.

We begin by comparing the evolution of the intensity of RPHNUC beams with conventional radially polarized partially coherent (RPPC) beams, which possess a uniform correlation structure.

Figure 1 shows the normalized intensity and corresponding cross-line of RPPC beams and RPHNUC beams at different distances in turbulence with different mode orders. We confirm that the beam profile of RPPC beams reduce from a dark hollow core to Gaussian distribution gradually in short propagation distance in turbulent atmosphere, as was studied in detail in Ref. [40]. This in turn indirectly indicates that the radial polarization structure is lost on propagation, as we will see later. In contrast, we find from Figs. 1(b) and (c) that, for two different mode orders, RPHNUC beams evolve in a nontrivial manner, manifesting rings of different sizes, sometimes multiple rings, at different intermediate distances, which is similar to its propagation properties in free space (see Fig. 1 in Ref. [28]), while at long propagation distance, the dark core of RPHNUC beams becomes shallower on propagation and eventually degrades to a Gaussian intensity profile. One can explain this phenomenon by the fact that the influence of turbulence can be neglected and the free-space diffraction plays a ring-shaped role at short propagation distance, thus the propagation properties of RPHNUC beams in turbulence is similar to those in free space. With a further increase of the propagation distance, the influence of turbulence accumulates and plays a dominant role, and the ring-shaped beam profile evolves into Gaussian distribution beam profile at long distances due to the isotropic influence of turbulence. It is worth noting that the evolution properties of the intensity are closely related to the mode order, the conversion from the ring-shaped distribution to Gaussian distribution becomes slower as the mode order increase, which suggests that RPHNUC beams with large mode order are less affected by turbulence.

In order to more clearly examine the evolution of the distribution of light intensity as it degenerates to a Gaussian distribution, Fig. 2 shows the ratio of the spectral intensity on the optical axis ($\rho = 0$) to the maximum intensity in the transverse plane. We find from Fig. 2(a) that the ratio of RPPC beams increase from 0 (i.e., intensity on optical axis is 0) to 1 (i.e., the beam profile reduces to a Gaussian distribution), gradually. The ratio of radially polarized NUC beams (with $m = 0$) increases rapidly over a short propagation distance, and then increase gradually to 1. Strikingly, when $m \neq 0$, i.e., RPHNUC beams, the ratio also increases rapidly over short distances, after which it increases gradually to a maximum, then it decreases to a fixed value, and then increases again very slowly. The phenomenon illustrates that the RPHNUC beams can keep the ring-shaped intensity distribution over much longer distances than RPPC beams with a conventional uniform correlation structure. Furthermore, RPHNUC beams with a larger mode
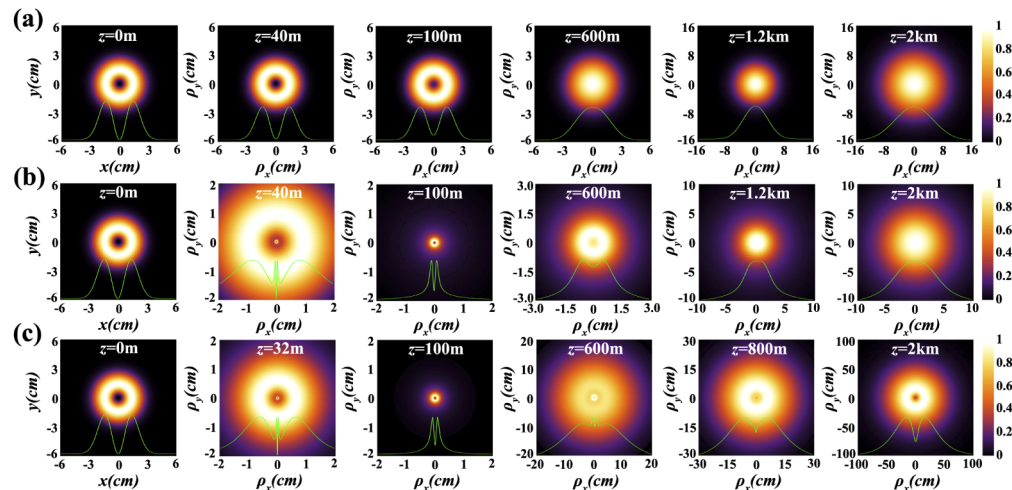

Fig. 1. Density plot of the normalized intensity of (a) RPPC beams and RPHNUC beams upon propagation in turbulence at different distances with different mode orders (b) $m = 0$ (c) $m = 1$.

order can keep the ring-shaped beam profile much better than a beam with lower mode order. Over short propagation distances, the value of the ratio first increases rapidly then increases gradually: we interpret this phenomenon as arising from the interplay between the intensities of the outer ring and inner ring and the effects from turbulence.
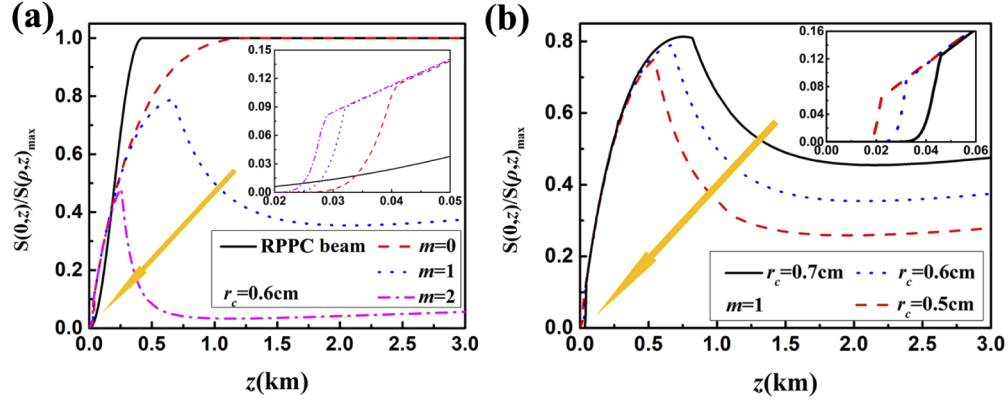

Fig. 2. Ratio of the spectral intensity on the optical axis ($\rho = 0$) to the maximum intensity in the transverse plane of RPHNUC beams versus the propagation distance z in turbulence for different values of (a) the mode order and (b) the coherence width.

Figure 2(b) shows the ratio of the spectral intensity in the optical axis to the maximum intensity in the transverse plane of RPHNUC beams versus the propagation distance z in turbulence for different values of the initial coherence width. One confirms that RPHNUC beams with low coherence can better maintain the ring-shaped beam profile at long propagation distance in turbulence; this is in contrast with RPPC beams, which typically lose their center ring more rapidly as coherence decreases. From these results, we can see that RPHNUC beams with low coherence display better turbulence resistance.

In Fig. 3, we illustrate (a) the normalized intensity distribution of RPHNUC beams on propagation, along with (b) its completely polarized part and (c) its completely unpolarized part for mode order $m = 1$. One finds from Fig. 3 that the dark core of intensity becomes shallower on propagation, due to the growth of an unpolarized bright spot, as shown in Fig. 3(c). The completely polarized part keeps its dark hollow beam profile invariant on propagation.

In order to observe the contribution of the completely polarized part of the intensity and the completely unpolarized part more clearly, in Fig. 4 we calculate the evolution of the normalized power of the completely polarized portion versus the propagation distance z in the turbulent atmosphere (the variation of the completely unpolarized portion is easy to get according to Fig. 4),

$$\eta^{(l)}(z) = \frac{\iint_{-\infty}^{\infty} \langle I^{(l)}(\boldsymbol{\rho}, z) \rangle \, d^2\boldsymbol{\rho}}{\iint_{-\infty}^{\infty} \langle I(\boldsymbol{\rho}, z) \rangle \, d^2\boldsymbol{\rho}}, \quad (l = p, u), \tag{28}$$

here, $\eta^{(p)}(z)$ and $\eta^{(u)}(z)$ denote the normalized powers of the completely polarized portion and the completely unpolarized portion of RPHNUC beams, respectively.

For the convenience of comparison, the corresponding results of RPPC beams are also shown in Fig. 4(a). As shown in Fig. 4(a), for RPPC beams, the power of the completely polarized portion decreases rapidly, i.e., it transits to the completely unpolarized portion on propagation in turbulence due to the influence of the initial spatial coherence and turbulence; we call this phenomenon coherence-induced and turbulence-induced depolarization, as predicted in Ref. [40]. One also confirms from Fig. 4(a), over short propagation distance, that the power of the completely polarized portion of RPHNUC beams decreases first, then increases, while with
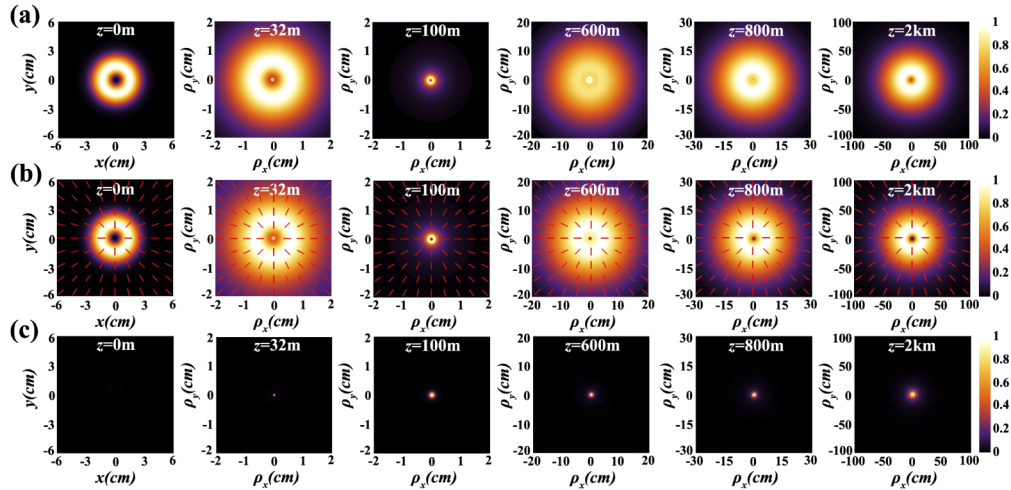
Fig. 3. Normalized intensity distributions of (a) RPHNUC beams, (b) its completely polarized part and (c) its completely unpolarized part with $m = 1$ on propagation in turbulence.
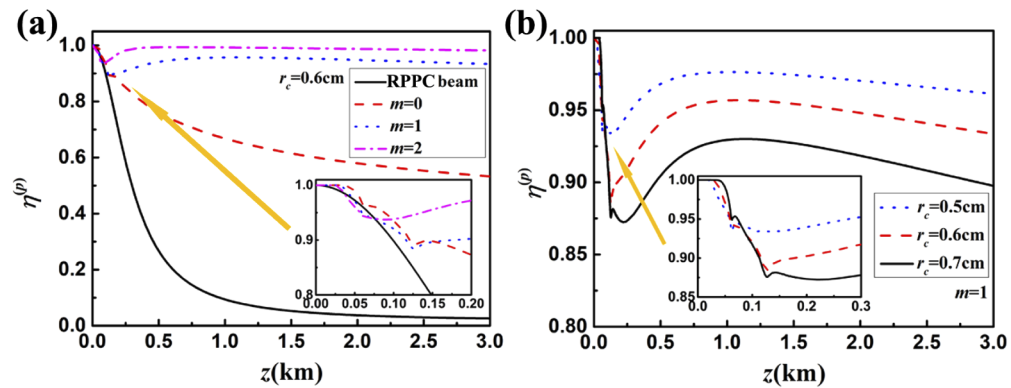

Fig. 4. Variation of the normalized powers of the completely polarized portion of RPHNUC beams versus the propagation distance z for (a) different values of the mode order and (b) the coherence width in turbulence.

increasing propagation distance, the power of the completely polarized portion decreases again. Furthermore, we find from Figs. 4(a) and (b), such beams with larger mode order and low coherence exhibit high power of the completely polarized portion over long propagation distance. We interpret the small fluctuation in the curve over short propagation distance as arising from the interplay between the intensities of the outer ring and inner ring and the effect from turbulence. Thus, one can say the non-uniform correlation structure plays a role of resisting coherence- and turbulence-induced depolarization of RPHNUC beams on propagation.

Now we analyze the degree of polarization (DOP) of RPHNUC beams on propagation in turbulence. It is to be noted that the chosen values of the mode order of RPHNUC beams have been increased to highlight the difference of the value of the DOP. We calculate in Fig. 5(a) that the DOP (cross line $\rho_y = 0$) of RPHNUC beams at propagation distance $z = 500\text{m}$ and in Fig. 5(b) the DOP of such beams at point $(5\text{mm}, 5\text{mm})$ versus the propagation distance z for different values of the mode order. For the convenience of comparison, the DOP of RPPC beams on propagation in turbulence also have been shown in Fig. 5. One finds from Fig. 5 that, upon propagation in the turbulent atmosphere, a dip appears in the distribution of the DOP. The dip of DOP of RPPC beams is obviously larger than which of RPHNUC beams, which means vector PCBs with non-uniform correlation structure exhibit much better resistance to depolarization than vector PCBs with uniform correlation structure. Furthermore, it is clear that the mode order affects the DOP on propagation in turbulence and usually the value of the DOP increases as the value of the mode order m increases, which means the mode order plays a role of anti-depolarization on propagation.
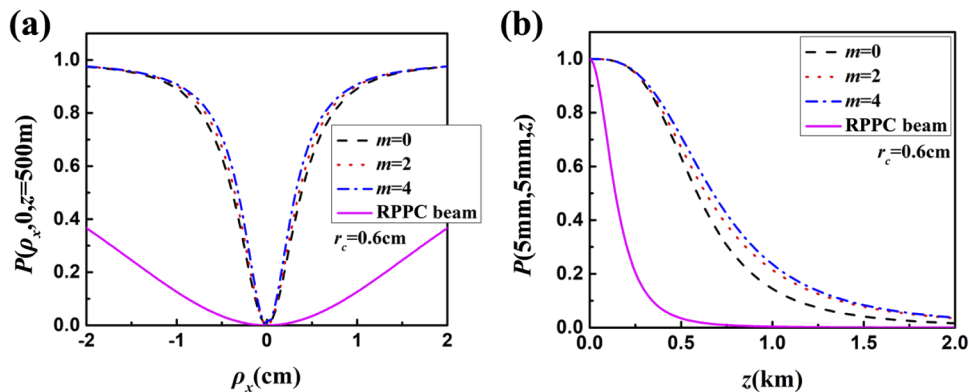

Fig. 5. DOP of RPHNUC beams (a) at $z = 500\text{m}$ (cross line $\rho_y = 0$); (b) at point $(5\text{mm}, 5\text{mm})$ versus the propagation distance z in turbulence for different mode order.

Figure 6 shows the evolution of the DOP of RPHNUC beams at certain propagation distance at $z = 500\text{m}$ versus the coordinate in ρ_x-axis and at certain point, again using a reference point $(5\text{mm}, 5\text{mm})$, versus the propagation distance in turbulence for different values of the correlation width of such beams. One confirms that the variation of the DOP on propagation in turbulence is also closely determined by the coherence width, and the DOP decreases more rapidly with high coherence, which means we can also adjust the coherence of RPHNUC beams to improve the resistance to depolarization induced by turbulence.
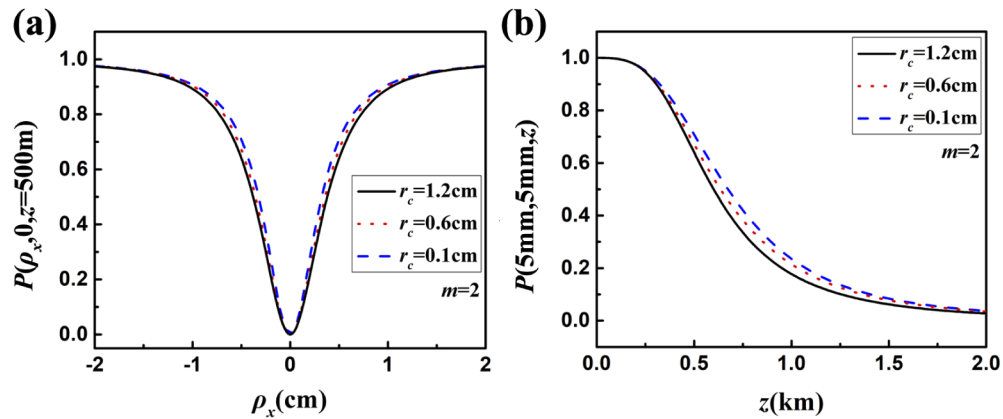
Fig. 6. DOP of RPHNUC beams (a) at $z = 500$m (cross line $\rho_y = 0$); (b) at point (5mm, 5mm) versus the propagation distance z in turbulence for different coherence width.

4. Summary and observations

We have studied the propagation properties of RPHNUC beams in turbulence and found that the propagation properties of such beams are quite different from those of vector PCBs with conventional uniform correlation structure in turbulence. We have showed that RPHNUC beams can better keep the original beam profile and polarization state over a greater propagation distance in turbulence, and RPHNUC beams with large mode order and/or low coherence are less affected by turbulence than such beams with small mode order and/or high coherence and vector conventional partially coherent sources.

It is worthwhile to say a few words about the physics that leads such beams to have their unusual properties. As seen from Eq. (3), the degree of coherence of a RPHNUC beam is azimuthally invariant, and depends only on the radial positions of the two observation points. As discussed in [28], the fluctuations in such a beam may be interpreted as a fluctuating wavefront curvature of the beam, which overall produces a broadened self-focus spot at long propagation distances. Since this curvature is radially symmetric, it does not distort the radial polarization of the beam or its axial intensity null. In contrast, the fluctuations of a Schell-model beam may be interpreted as a fluctuating tilt of the beam, which distorts both the polarization distribution of the beam as well as the position of the axial zero, causing both to disappear on propagation.

We have also seen that higher-order modes maintain their dark core over longer distances on propagation than lower-order modes. For higher-order modes, the beam self-focuses at a closer distance than lower-order modes, which indicates it spreads more rapidly over long propagation distances. This can be seen, for instance, in the rightmost panels of Fig. 1, and the plot ranges used. Because the beam components are propagating at a much larger angle with respect to the beam axis, the turbulence is less likely to scatter them back along the axis. This suggests a trade-off: one can maintain a dark hollow core of RPHNUC beams over longer distances, but at the cost of more overall beam spreading.

Our results show that the beams with combination of polarization and non-uniform correlation structure show more resistance to turbulence, and have a number of degrees of freedom, polarization and/or non-uniform coherence, which can be tailored for the individual application needs. This flexibility can be used to improve the characteristics of beams in FSO communications.

Funding

Disclosures

The authors declare no conflicts of interest.

References

1. J. Baumgartl, M. Michael, and D. Kishan, "Optically mediated particle clearing using Airy wavepackets," Nat. Photonics **2**(11), 675–678 (2008).
2. V. Garceschavez, D. Mcgloin, H. Melville, W. Sibbett, and K. Dholakia, "Simultaneous micromanipulation in multiple planes using a self-reconstructing light beam," Nature **419**(6903), 145–147 (2002).
3. M. P. Lavery, F. C. Speirits, S. M. Barnett, and M. J. Padgett, "Detection of a Spinning Object Using Light's Orbital Angular Momentum," Science **341**(6145), 537–540 (2013).
4. Z. Qiao, Z. Wan, G. Xie, J. Wang, and D. Fan, "Multi-vortex laser enabling spatial and temporal encoding," PhotoniX **1**(1), 13–14 (2020).
5. L. C. Andrews and R. L. Phillips, *Laser Beam Propagation through Random Media* (SPIE, 2005).
6. G. Gbur, "Partially coherent beam propagation in atmospheric turbulence," J. Opt. Soc. Am. A **31**(9), 2038–2045 (2014).
7. F. Wang, X. Liu, and Y. Cai, "Propagation of partially coherent beam in turbulent atmosphere: a review (Invited review)," Prog. Electromagnetics Res. **150**, 123–143 (2015).
8. Y. Cai, Y. Chen, J. Yu, X. Liu, and L. Liu, "Generation of partially coherent beams," Prog. Opt. **62**, 157–223 (2017).
9. Y. Chen, S. A. Ponomarenko, and Y. Cai, "Experimental generation of optical coherence lattices," Appl. Phys. Lett. **109**(6), 061107 (2016).
10. J. C. Leader, "Intensity fluctuations resulting from partially coherent light propagating through atmospheric turbulence," J. Opt. Soc. Am. **69**(1), 73–84 (1979).
11. V. A. Banakh and V. M. Buldakov, "Effect of the initial degree of spatial coherence of a light beam on intensity fluctuations in a turbulent atmosphere," Opt. Spectrosc. **55**(4), 423–426 (1983).
12. R. Lin, H. Yu, X. Zhu, L. Liu, G. Gbur, Y. Cai, and J. Yu, "The evolution of spectral intensity and orbital angular momentum of twisted Hermite Gaussian Schell model beams in turbulence," Opt. Express **28**(5), 7152–7164 (2020).
13. O. Korotkova, L. C. Andrews, and R. L. Phillips, "Model for a partially coherent Gaussian beam in atmospheric turbulence with application in Lasercom," Opt. Eng. **43**(2), 330–341 (2004).
14. G. Gbur and E. Wolf, "Spreading of partially coherent beams in random media," J. Opt. Soc. Am. A **19**(8), 1592–1598 (2002).
15. T. Shirai, A. Dogariu, and E. Wolf, "Mode analysis of spreading of partially coherent beams propagating through atmospheric turbulence," J. Opt. Soc. Am. A **20**(6), 1094–1102 (2003).
16. F. Gori and M. Santarsiero, "Devising genuine spatial correlation functions," Opt. Lett. **32**(24), 3531–3533 (2007).
17. F. Gori, V. R. Sánchez, M. Santarsiero, and T. Shirai, "On genuine cross-spectral density matrices," J. Opt. A: Pure Appl. Opt. **11**(8), 085706 (2009).
18. R. Chen, L. Liu, S. Zhu, G. Wu, F. Wang, and Y. Cai, "Statistical properties of a Laguerre- Gaussian Schell-model beam in turbulent atmosphere," Opt. Express **22**(2), 1871–1883 (2014).
19. J. Yu, Y. Chen, L. Liu, X. Liu, and Y. Cai, "Splitting and combining properties of an elegant Hermite-Gaussian correlated Schell-model beam in Kolmogorov and non-Kolmogorov turbulence," Opt. Express **23**(10), 13467–13481 (2015).
20. M. Tang and D. Zhao, "Propagation of multi-Gaussian Schell-model vortex beams in isotropic random media," Opt. Express **23**(25), 32766–32776 (2015).
21. X. Liu, J. Yu, Y. Cai, and S. A. Ponomarenko, "Propagation of optical coherence lattices in the turbulent atmosphere," Opt. Lett. **41**(18), 4182–4185 (2016).
22. F. Wang, J. Li, G. Martinez-Piedra, and O. Korotkova, "Propagation dynamics of partially coherent crescent-like optical beams in free space and turbulent atmosphere," Opt. Express **25**(21), 26055–26066 (2017).
23. Z. Tong and O. Korotkova, "Nonuniformly correlated light beams in uniformly correlated media," Opt. Lett. **37**(15), 3240–3242 (2012).
24. Y. Gu and G. Gbur, "Scintillation of nonuniformly correlated beams in atmospheric turbulence," Opt. Lett. **38**(9), 1395–1397 (2013).
25. H. Lajunen and T. Saastamoinen, "Non-uniformly correlated partially coherent pulses," Opt. Express **21**(1), 190–195 (2013).
26. J. Yu, F. Wang, L. Liu, Y. Cai, and G. Gbur, "Propagation properties of Hermite non-uniformly correlated beams in turbulence," Opt. Express **26**(13), 16333–16343 (2018).

27. J. Yu, Y. Cai, and G. Gbur, "Rectangular Hermite nonuniformly correlated beams and its propagation properties," Opt. Express **26**(21), 27894–27906 (2018).
28. J. Yu, X. Zhu, S. Lin, F. Wang, G. Gbur, and Y. Cai, "Vector partially coherent beams with prescribed non-uniform correlation structure," Opt. Lett. **45**(13), 3824–3827 (2020).
29. Y. Gu, O. Korotkova, and G. Gbur, "Scintillation of nonuniformly polarized beams in atmospheric turbulence," Opt. Lett. **34**(15), 2261–2263 (2009).
30. J. Zhang, S. Ding, and A. Dang, "Polarization property changes of optical beam transmission in atmospheric turbulent channels," Appl. Opt. **56**(18), 5145–5155 (2017).
31. C. Wei, D. Wu, C. Liang, F. Wang, and Y. Cai, "Experimental verification of significant reduction of turbulence-induced scintillation in a full Poincare beam," Opt. Express **23**(19), 24331–24341 (2015).
32. F. Wang, X. Liu, L. Liu, Y. Yuan, and Y. Cai, "Experimental study of the scintillation index of a radially polarized beam with controllable spatial coherence," Appl. Phys. Lett. **103**(9), 091102 (2013).
33. H. Wang, D. Liu, and Z. Zhou, "The propagation of radially polarized partially coherent beam through an optical system in turbulent atmosphere," Appl. Phys. B **101**(1-2), 361–369 (2010).
34. J. Yu, Y. Huang, F. Wang, X. Liu, G. Gbur, and Y. Cai, "Scintillation properties of a partially coherent vector beam with vortex phase in turbulent atmosphere," Opt. Express **27**(19), 26676–26688 (2019).
35. C. Sun, X. Lv, B. Ma, J. Zhang, D. Deng, and W. Hong, "Statistical properties of partially coherent radially and azimuthally polarized rotating elliptical Gaussian beams in oceanic turbulence with anisotropy," Opt. Express **27**(8), A245–A256 (2019).
36. Z. Song, Z. Han, J. Ye, Z. Liu, S. Liu, and B. Liu, "Propagation properties of radially polarized multi-Gaussian Schell-model beams in oceanic turbulence," J. Opt. Soc. Am. A **36**(10), 1719–1726 (2019).
37. E. Wolf, *Introduction to the Theory of Coherence and Polarization of Light* (Cambridge University, 2007).
38. O. Korotkova, M. Salem, A. Dogariu, and E. Wolf, "Changes in the polarization ellipse of random electromagnetic beams propagating through the turbulent atmosphere," Waves Random Complex Media **15**(3), 353–364 (2005).
39. I. Toselli, L. C. Andrews, R. L. Phillips, and V. Ferrero, "Free-space optical system performance for laser beam propagation through non-Kolmogorov turbulence," Opt. Eng. **47**(2), 026003 (2008).
40. X. Peng, L. Liu, J. Yu, X. Liu, Y. Cai, Y. Baykal, and W. Li, "Propagation of a radially polarized twisted Gaussian Schell-model beam in turbulent atmosphere," J. Opt. **18**(12), 125601 (2016).